Cancer Chemotherapy and Pharmacology (2019) 84:551–559
https://doi.org/10.1007/s00280-019-03870-x

ORIGINAL ARTICLE

Identification of dinactin, a macrolide antibiotic, as a natural product-based small molecule targeting Wnt/β-catenin signaling pathway in cancer cells

Aehtesham Hussain[1,3] · Mohd Saleem Dar[1,2,4] · Nasima Bano[1,2] · Md Mehedi Hossain[1,2] · Rafia Basit[1,2] · Aadil Qadir Bhat[1,2] · Mushtaq A. Aga[5] · Sabeena Ali[3] · Qazi Parvaiz Hassan[1,3] · Mohd Jamal Dar[1,2]

Received: 17 November 2018 / Accepted: 10 May 2019 / Published online: 25 May 2019

Abstract

Purpose Despite the fact that hyper-activation of Wnt/β-catenin signaling pathway has been seen in many cancers, including liver, colorectal and lung carcinoma, no small molecule inhibitors are available that specifically target this pathway. In this study, we analyzed the impact of dinactin (DA), an antibiotic ionophore produced by *Streptomyces* species, as an effective small molecule targeting Wnt/β-catenin signaling pathway in cancer cells.

Methods We performed MTT assays to investigate cell viability and proliferation after exposure to small molecules. Protein expression analysis was carried out by western blotting. Top-Flash reporter assays were used to score for β-catenin signaling and cell cycle analysis was carried out by flow cytometry.

Results In the first set of experiments, DA was seen to selectively inhibit the proliferation of HCT-116 and HepG2 cancer cells, unlike HEK-293 cells (a low tumorigenic cell line), in apoptosis-independent manner. Further, DA was seen to block the G1/S progression and decrease the expression of cyclin D1 in cancer cells. Since cyclin D1 is the downstream target gene of Wnt/β-catenin signaling, we examined the impact of DA on TCF-dependent β-catenin activity using Top-Flash reporter assay. Interestingly, DA significantly decreased Top-Flash activity at lower nano-molar concentrations when compared with salinomycin in HCT-116 and HepG2 cells.

Conclusion We report the identification of dinactin as a natural product-based small molecule that effectively blocks the Wnt/β-catenin signaling pathway in cancer cells at nano-molar concentration. We anticipate that DA could be developed as a novel drug for anti-cancer therapy and for the management of neuropathic pain.

Keywords Antibiotic · Ionophore · Wnt/β-catenin signaling · Apoptosis · Anti-cancer agents · HCT-116 and HepG2 cells

Introduction

Most of the antibiotics isolated from *Streptomyces* usually target bacterial DNA replication, protein synthesis machinery or inhibit cell wall synthesis [1]. However, many classes of antibiotics such as, salinomycin, bleomycins, enediynes

Aehtesham Hussain and Mohd Saleem Dar contributed equally to this work.

Electronic supplementary material The online version of this article (https://doi.org/10.1007/s00280-019-03870-x) contains supplementary material, which is available to authorized users.

✉ Qazi Parvaiz Hassan
qphassan@iiim.ac.in

✉ Mohd Jamal Dar
jamal@iiim.ac.in

[1] Academy of Scientific and Innovative Research, New Delhi, India

[2] Cancer Pharmacology Division, CSIR – Indian Institute of Integrative Medicine, Jammu Tawi 180001, India

[3] Microbial Biotechnology Division, CSIR – Indian Institute of Integrative Medicine, Sanat Nagar, Srinagar, Jammu and Kashmir 190005, India

[4] Present Address: Department of Biochemistry, Purdue University, West Lafayette, IN 47907-2063, USA

[5] Medicinal Chemistry Division, CSIR – Indian Institute of Integrative Medicine, Jammu Tawi, Jammu and Kashmir 180001, India

and mitomycins have strong antitumor activities [2]. We isolated dinactin (DA), a macrolide antibiotic, from *Streptomyces puniceus* AS13 and examined it for various activities [3]. The macrotetrolide antibiotics isolated from *Streptomyces* species are primarily considered as ionophoric compounds but have also been reported to show different bioactivities [4]. The nonactin, an ionophore molecule from macrotetrolide family [5, 6] has been found as efflux pump inhibitor in drug-resistant cancers [7]. The antitumor property of macrotetrolides and mechanism of their antitumor action is not fully explored yet. Salinomycin, a carboxylic polyether antibiotic ionophore isolated from *Streptomyces albus*, is reported to show strong anti-cancer properties [8, 9]. Salinomycin is shown to induce cell death in cancer cells such as breast, lung and gastric cancers, etc. Lu et al. [8] showed that salinomycin inhibits Wnt signaling and induces apoptosis in chronic lymphocytic leukemia cells. Wnt/β-catenin signaling plays defining roles in cell proliferation, differentiation and in embryonic development and maintenance of organs and tissues during various stages of development. Aberrant activation of Wnt/β-catenin signaling pathway is preferentially involved in progression of different types of cancers including colon, liver, lung and ovarian ones [10–12]. Recently, studies on Wnt/*β*-catenin signaling pathway has been shown to play critical roles in the induction and maintenance of chronic neuropathic pain [13, 14]. Accordingly, small molecules targeting Wnt/β-catenin pathway have gained immense promise for the development of anti-cancer drugs, and for the management of neuropathic pain.

Here in this study, we report the identification of dinactin as an effective cytostatic anti-cancer agent that inhibits the proliferation of human cancers without inducing cell death. In addition, dinactin showed a strong inhibitory effect on TCF-dependent β-catenin-mediated signaling activity in HCT-116 and HepG2 cells indicating that dinactin could be developed as an anti-cancer drug, and an effective agent for the management of neuropathic pain.

Materials and methods

Chemicals, antibodies and reagents

Anti-parp (SC-8007), anti-caspase-3 (SC-271028), anti-cyclin D1 (SC-753), anti-cyclin B1 (SC-752), anti-p21 (SC-6246), HRP-conjugated anti-mouse (SC-2005) and anti-goat (SC-2354) antibodies were procured from Santa Cruz Biotechnology; anti-β-actin (Cat. No., 4970S) antibody was procured from Cell Signaling Technology (Danvers, MA). Salinomycin, paraformaldehyde, propidium iodide, DAPI 3-(4,5-dimethylthiazole-2-yl)-2,5-diphenyltetrazolium bromide (MTT), 2′,7′-dichlorofluorescin diacetate (H2DCFDA) dye, DMSO, proteinase K, eukaryotic protease inhibitor cocktail, growth medium (RPMI-1640 and DMEM), fetal bovine serum, phosphate buffer saline (PBS), trypsin–EDTA, penicillin, streptomycin were purchased from Sigma. Dinactin was isolated from culture broth of *Streptomyces puniceus* strain AS08 as described previously with complete spectral description (the molecule was isolated as sticky brown oil HR-ESIMS: m/z 764).

Cell culture, growth conditions and treatment

HEK-293 and HCT-116 cells were obtained from American Type Culture Collection (ATCC), while HepG2 cells were obtained from Sigma. HEK-293 and HepG2 cells were grown in DMEM, and HCT-116 cells were grown in RPMI-1640 containing 10% FBS in CO_2 incubator with 5% CO_2 and 98% humidified conditions at 37 °C. Cells were treated with different doses of test compounds dissolved in DMSO while the DMSO was used as control for the experiments.

Cell proliferation by MTT assay

Cell proliferation was determined by using MTT assay. Briefly, 6000–8000 cells/well were seeded in 96-well plate, and next day, were treated with different concentrations of test compounds and incubated for 24, 48 and 72 h at 37 °C in CO_2 incubator. After 24, 48 and 72 h post-treatment, 20 µl of MTT solution (2.5 mg/ml) was added to each well to form the formazan crystals and incubated for 4 h at 37 °C. Media was removed and DMSO (150 µl/well) was added to dissolve the crystals, and the absorbance was recorded at 570 nm in the micro-plate reader. The values were later evaluated to calculate the IC_{50} of the molecules by using GraphPad Prism5 software.

Assessment of nuclear morphology

HCT-116 cells (0.3×10^6) were seeded in 6-well plates and grown overnight at 37 °C in CO_2 incubator. Next day the cells were treated with different concentrations of DA and grown further for 24 h. Then, cells were trypsinized and centrifuged at 1600 rpm for 5 min at 4 °C and washed with PBS. Cells were then fixed with methanol for 30 min at 4 °C and finally suspended in 500 µl PBS. 1 µg/ml DAPI, a nuclear stain, was added to cell suspension for 10 min followed by centrifugation. The pellet was resuspended in 50 µl of mountant fluid (PBS:glycerol in the ratio 1:1). For microscopy, 10 µl cell suspension was spread on glass slide, coverslips were placed carefully and sealed with nail polish under dark conditions [15]. Nuclear morphological alterations were observed using inverted fluorescence microscope (Olympus 1 × 70, magnification 30×) by UV excitation.

Measurement of intracellular reactive oxygen species (ROS)

ROS generation was measured using DCFH-DA [16]. Briefly, HCT-116 cells seeded in 96-well plates (5000–10000 cells/well) were treated with different concentrations of DA for 24 h. Thereafter, cells were washed with PBS and treated with 10 µM DCFH-DA diluted in RPMI medium for 30 min (at 37 °C, 5% CO_2). The cells were washed three times with PBS and finally resuspended in PBS (200 µl) and kept in dark for 30 min. Fluorescence intensity of DCFH-DA was measured at an excitation wavelength of 504 nm and emission wavelength of 529 nm.

Preparation of whole cell lysates for immunoblotting

HCT-116 and HepG2 cells (0.3×10^6/well) seeded in 6-well plates were treated with different concentrations of test compounds. After 24 h treatment, the cells were harvested and washed with cold PBS. The cell pellets were resuspended in cold RIPA lysis buffer (50 mM Tris–HCl, 150 mM NaCl, 5 mM EDTA, 1% triton X-100, 0.1% SDS, 30 mM Na_2HPO_4, 50 mM NaF, 0.5 mM $NaVO_4$, 2 mM PMSF supplemented with 1% protease inhibitor cocktail) for 40 min with a vortex of 10 s after every 10 min on ice. The cell lysates were centrifuged at 14000 rpm at 4 °C for 20 min. Supernatants transferred to fresh tubes were estimated for protein concentration by Bradford assay. After determining the protein concentration, the samples were denatured in 5X lysis buffer (100 mM Tris–HCl, 4% SDS, 0.1% bromophenol blue, 20% glycerol and 200 mM β-mercaptoethanol) for 10 min at 100 °C, and the lysates were stored at − 80 °C for further use.

Western blotting analysis

Equal quantity of proteins (70 µg) were resolved on SDS-PAGE (8-12%) at 100 V for 2–3 h, followed by electro-transfer to PVDF membrane (Immobilon-P Transfer Membrane Millipore) at 110 V for 2 h at chilled conditions. Membranes were either blocked with 5% BSA or skimmed milk (fat free) in TBST (20 mM Tris–HCl pH 7.4, 150 mM NaCl, 0.1% Tween 20) solution for 1 h at room temperature. Blocked membranes were incubated with respective primary antibodies at dilution of 1:500–1:1000 overnight at 4 °C on a dancing rocker. Next day, the blots were washed three times with TBST buffer after 5 min interval. This was followed by incubation with corresponding (anti-mouse or anti-rabbit or anti-goat) secondary antibody (with conjugated Horseradish Peroxidase tag) for 1–3 h on a dancing rocker. The blots were then again washed three times with TBST, each for 5 min. Blots, in dark room, were poured with enhanced chemiluminescence (ECL) substrate and the signal was captured on X-ray film in a hypercassette. The X-ray film were developed in developing solution till the signal appears, and immediately fixed in fixing solution under dark conditions. The bands are analyzed by Image J 1.49 software for densitometric analysis.

Cell cycle analysis

Cells (0.3×10^6/well) were grown in 6-well plates and treated with different concentrations of DA for 24 h, the cells were harvested by centrifuging at 1000 rpm for 5 min at 4 °C, followed by washing with PBS. The cells were then fixed in 70% ethanol and kept overnight at 4 °C. Next day, the cell suspension was centrifuged and washed with ice-cold PBS. Cells were resuspended in 200 µl of PBS, digested with 100 µg/ml RNase (at 37 °C for 90 min). The cells were then stained with propidium iodide (PI, 10 µg/ml) immediately and incubated in dark for 30 min. Finally PBS was added to make final volume to 500 µl. All the samples were analyzed for cell cycle by using FACS BD Calibur. Data was analyzed by using MOLT FIT software.

TOP-Flash reporter assays

Wnt/β-catenin-mediated transcription was determined by TOP-Flash reporter assay. Briefly, cells (0.3×10^6 cells/well) were seeded in 6-well plates and grown overnight at 37 °C in CO_2 incubator. Next day, the cells were transfected with plasmids expressing TOP or FOP and Renilla plasmids using Lipofectamine 2000 (Invitrogen). Herein, the Lipofectamine was incubated with serum-free medium in a centrifuge tube in the laminar hood for 5 min and added to plasmid DNA in a drop-wise manner to form a lipo–plasmid mix, which was incubated for 30 min. In the meantime, the overnight media of cells was replaced by serum-free media, and exactly after 30 min the plasmid–lipo mix was added to cells in a drop-wise manner, and grown at 37 °C in CO_2 incubator. After 4 h of transfection, cells were treated with DMSO and different concentrations of DA, and grown overnight at 37 °C in CO_2 incubator. After 24 h post-transfection, cells were washed with PBS and lysed with 1X Lysis buffer (Promega). The lysates were pelleted by mini spin, and the supernatant was used for measuring the luciferase activity. Relative luciferase activity of cells was measured using the Dual-Luciferase Reporter Assay System (Promega) according to the manufacturer's instructions. The relative luciferase activities (TOP-Flash values) of each well were calculated by determining the ratio of the Luciferase signal to Renilla signal. Three independent transfections were carried out in duplicate for each of the concentrations tested.

NF-κB reporter assay

NF-κB reporter assays were performed in HepG2 cells. Briefly, cells (at 0.3×10^6 cells/well) were transfected with 800 ng of NF-κB or pGL3 vector and 200 ng of Renilla DNA. Four hours after transfection, cells were treated with DA and supplemented with complete media. Cells were processed and luciferase readings were measured in the similar way as discussed for TOP-Flash Reporter assays. Each condition was assayed in triplicate, and each experiment was carried out at least three times.

Statistical analysis

MOLT FIT, Adobe Photoshop 7.0, ImageJ, and GraphPad Prism5 software were used for data analysis. Student's *t* test and analysis of variance (ANOVA) were used to evaluate the differences between means. Data are expressed as mean ± SEM. Statistical significance was accepted at $P < 0.05$.

Results

Dinactin shows anti-proliferative activity against the cancer cells in apoptosis-independent manner

Streptomycetes synthesize compounds that are reported to show antibacterial, anti-inflammatory, antifungal, and antitumor activity [17, 18]. Recently, we isolated dinactin from *streptomyces puniceus* and characterized its structure [3]. Since, DA is an ionophore antibiotic, we got interested to study its antitumor activities in order to understand its mode of action. In our previous study, we analyzed the effect of DA (0.1–100 µM) against a panel of cancer cell lines, including PC-3, MIA PaCa-2, MOLT-4, HL-60, OVCAR-5, HCT-116, MCF-7, T47D, A549 and HepG2 cells, to investigate its relative growth inhibition using MTT assay. Interestingly, DA showed marked inhibition of HCT-116 cell growth with an IC_{50} of 1.1 µM [3]. Although DA was found to be a profound inhibiter of cancer cells, it showed no significant impact on the growth of non-tumor cells (HEK-293 cells). In order to evaluate whether the anti-proliferative effect of DA is mediated through apoptosis in HCT-116 cells, we carried out the immunoblotting to check the expression of apoptotic markers. Interestingly, DA treatment of HCT-116 cells for 48 h could not induce the cleavage of PARP-1 and caspase-3 proteins, the hallmark proteins of intrinsic and extrinsic pathways of apoptosis, respectively (Fig. 1a). Also, no cleavage of PARP or caspase-3 was detected at with higher doses of DA (5 µM) treatment in HCT-116 cells. We then analyzed the nuclear morphology of HCT-116 cells by DAPI staining, and found that indeed there is no nuclear shrinking or apoptotic nuclei upon the DA treatment even up to 5 µM concentrations (Fig. 1b). Next, owing to antimicrobial nature of DA, the involvement of the ROS-dependent damage within the cells was determined using 2′,7′-dichlorofluorescin diacetate (DCF-DA). Although we found production of intracellular ROS in comparison to untreated control, it was concentration independent and did not induce cell death as determined by microscopy (Supplementary Fig. 1). Taken together, these results suggested that anti-proliferative role of DA in cancer cells is occurring independent of apoptosis.

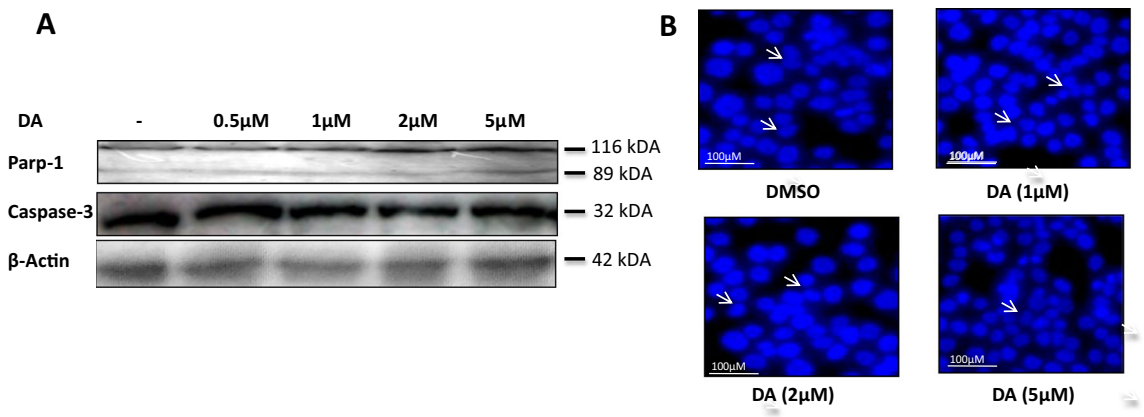

Fig. 1 Analyzing induction of apoptosis by dinactin in HCT-116 cells. **a** HCT-116 cells were treated with dinactin at indicated concentrations for 24 h, whole cell lysates were analyzed for cleaved PARP-1 and caspase-3 by western blot. β-actin was used as a loading control. (data are representative of three independent experiments). **b** HCT-116 cells were treated with dinactin at indicated concentrations and nuclear staining was done with DAPI. In treated cells no nuclear shrinking or apoptotic nuclei was observed

Dinactin induces cell cycle arrest at G1/S phase in HCT-116 cells

Deregulation in the cell cycle control is one of the fundamental characteristics of cancers [18]. So, to examine the mechanism(s) through which DA blocks cellular proliferation, we determined its effect on cell cycle progression. HCT-116 cells were treated with various concentrations of DA and analyzed using flow cytometry. We observed significant accumulation of HCT-116 cells in G1 phase (Fig. 2a, b). In untreated HCT-116 cells, 45–50% population were found in G1 phase, 43.34 in S phase and 10.05 in G2 phase, while as in DA-treated HCT-116 cells, 75–85% of population were in G1 phase, thus inhibiting the progression of cells to S phase. The cell cycle arrest at G1/S phase was observed even at 0.5 µM for 24 h, showing the potency of DA as an anticancer molecule. These results indicate that DA treatment induces G1 phase arrest in HCT-116 cells, thus inhibiting the progression of cells to S phase.

Dinactin decreased cyclin D1 expression in a concentration-dependent manner

Cyclins are known to regulate the cell cycle progression, and their relative levels help to understand cell cycle phases. Thus, to delineate the molecular mechanism of DA-mediated G1 arrest, we explored the expression of cyclins by western blotting. Upon the treatment of HCT-116 cells with DA, we observed a marked decrease in the expression of cyclin D1 in a dose-dependent manner while there was no significant change in the expression levels of cyclin E (Fig. 3a, b). p21 is a negative regulator of cyclin D1, thus negatively regulates the G1 transition. Interestingly, the immunoblotting and densitometry analysis of p21 showed a significant increase in the levels of p21 expression in a dose–dependent manner suggesting that DA modulates G1 cell cycle regulatory proteins in HCT-116 cells which subsequently leads to cell cycle arrest at G1/S phase that corresponds to inhibition of cell proliferation.

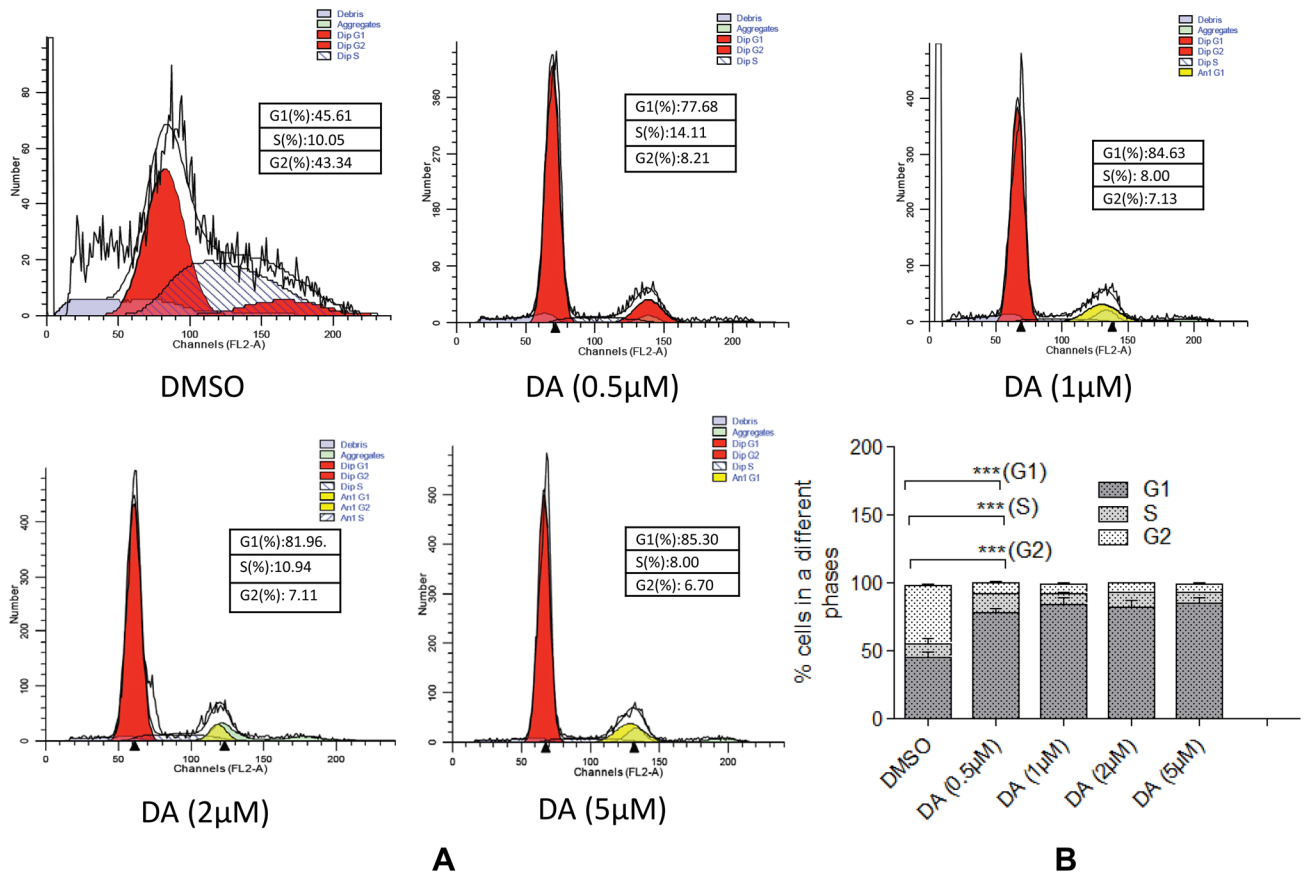

Fig. 2 Effect of dinactin (DA) on cell cycle phase distribution in HCT-116 cells. **a** HCT-116 cells were treated with indicated concentrations of dinactin for 24 h. Cells were stained with PI and analyzed for cell populations using flow cytometry as described in "Materials and Methods". Data are representative of one of the three similar experiments. **b** Bar graph represents the percentage of cells in various phases of cell cycle. For analysis, Student's *t* test was used, bar graphs are mean ± s.e.m. In vitro data are the means of three independent experiments. ***$P < 0.001$

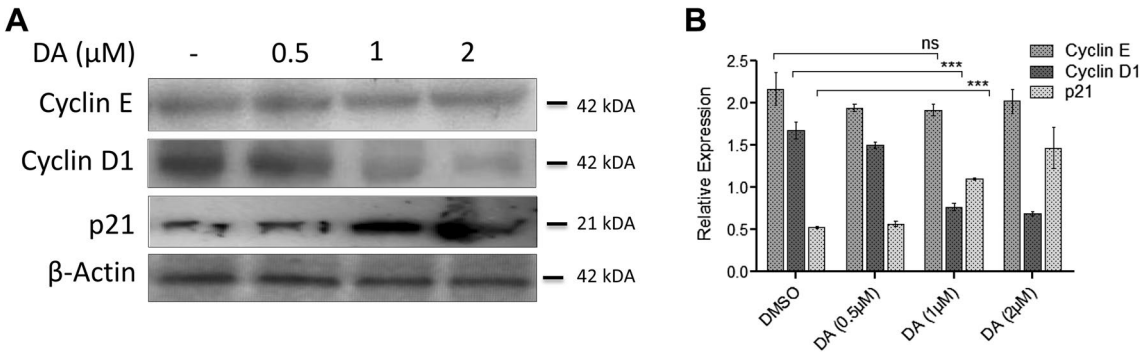

Fig. 3 **a** Influence of dinactin (DA) on the expression of proteins involved in cell cycle regulation in HCT-116 cells. HCT-116 cells were treated with the indicated concentrations of dinactin for 24 h. Whole cell protein lysates were prepared for western blotting and the detection of the indicated proteins. β-actin was used as an internal loading control. Data are representative of one of two similar experiments. **b** Densitometric analysis of cyclin D1, cyclin E, p21 protein expression in treated HCT-116 cells. All the experiments were done in triplicates. For analysis one-way ANOVA was used, bar graphs are mean ± s.e.m. $***P < 0.001$, and ns means non-significant

Dinactin inhibits Wnt/β-catenin signaling in HCT-116 and in HepG2 cells at nano-molar concentrations

Since DA treatment resulted in a significant decrease in the levels of cyclin D1, a downstream target protein of Wnt/β-catenin pathway, we speculated the reduced levels of cyclin D1 are due to the inhibition of Wnt/β-catenin signaling by DA treatment in these cells. Thus, we performed the Top-Flash luciferase reporter assay that monitors the β-catenin-mediated transcription of target genes. Interestingly, significant inhibition of Top-Flash activity upon DA treatment in HCT-116 cells was observed, DA at 500 nM inhibited β-catenin transcriptional activity to half in HCT-116 cells (Fig. 4a). We demonstrated in our recent study that HepG2 cells harbor a β-catenin deletion responsible for its enhanced β-catenin-mediated transcriptional activity [19, 20]. This leads us to explore the potential of DA as an inhibitor of hyperactivated β-catenin signaling in HepG2 cells as well. We performed Top-Flash reporter assay in presence of DA and salinomycin, a known ionophore antibiotic which inhibits Wnt/β-catenin signaling, in HepG2 cells, a standard cell line for assessing β-catenin signaling activity [21]. While comparing the potential of DA and salinomycin to inhibit the Wnt/β-catenin signaling, DA inhibited the Top-Flash reporter activity at lower doses than salinomycin in HepG2 cells. While salinomycin at 20 μM inhibited the Wnt/β-catenin activity to half, DA showed almost similar effect at 100 nM in HepG2 cells, making it a suitable natural product-based molecule of choice to target the hyperactive Wnt/β-catenin signaling pathway in different cancers (Fig. 4b). In order to validate these results, we performed these experiments using NF-κB reporter assay as well. Interestingly, no change in NF-κB reporter activity was observed upon DA treatment at different concentrations, indicating that DA specifically inhibits Wnt/β-catenin signaling in HepG2 cells (Supplementary Fig. 2).

Inhibition of Wnt/β-catenin by dinactin in HepG2 cells occurs through a similar mechanism like in HCT-116 cells

Since DA was involved in inhibiting Wnt/β-catenin signaling in HepG2 cells, we also explored the mechanism of its inhibition in these cells. Interestingly, like in HCT-116 cells, DA inhibited proliferation of HepG2 in an apoptosis-independent manner, as demonstrated by immunoblotting of the apoptotic marker proteins (Fig. 5a). Similarly, DA-treated HepG2 cells were unable to enter into the S phase of cell cycle due to the G1 arrest. Nearly 70% of the cells were arrested in G1 phase at 100 nM dose of DA (Fig. 5c, Supplementary Fig. 3). Also, the cell cycle arrest was mediated through the down-regulation of cyclin D1 as confirmed by immunoblotting (Fig. 5d). Taken together, the DA-mediated inhibition of the Wnt/β-catenin signaling causes the down-regulation of cyclin D1 which results in arresting these cells in G1 phase of cell cycle thus inhibiting their proliferation.

Discussion

The highly conserved Wnt/β-catenin signaling pathway is closely connected to development of cancers and is involved in the management of neuropathic pain [13, 14, 22]. β-Catenin, the pivotal element in the canonical Wnt signaling pathway is considered as an attractive therapeutic target for carcinogenesis [23, 24]. Upon ligand-mediated activation of canonical Wnt pathway, β-catenin proteins is stabilized and then it translocates into the nucleus where it acts as a transcriptional co-activator and binds to transcription

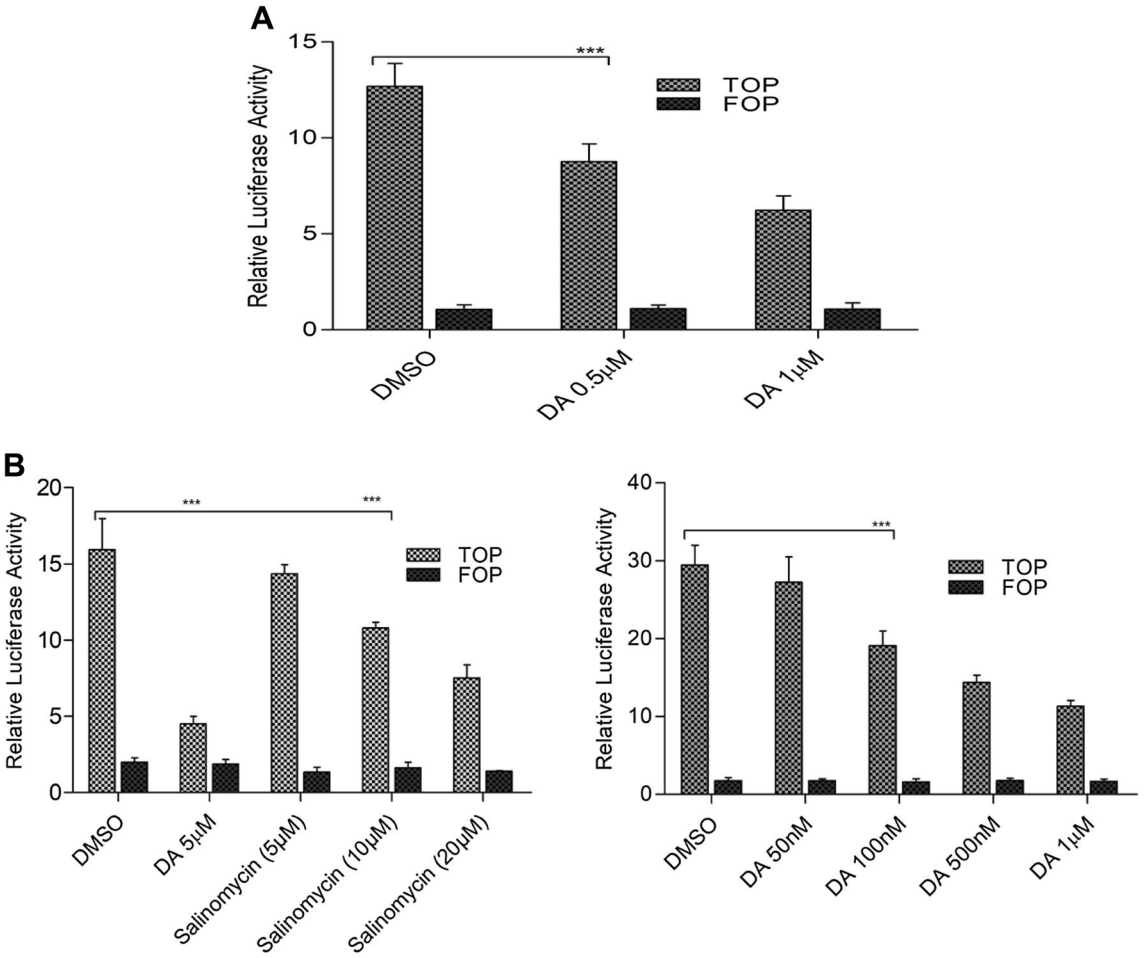

Fig. 4 Dinactin inhibits β-catenin/Wnt signaling pathway in HCT-116 and HepG2 cells. Reporter assays were performed using TOP-Flash luciferase assay. TOP-Flash activity after 24 h was determined upon co-transfection of TOP-Flash or FOP-Flash and Renilla plasmids into in **a** HCT-116 cells and **b** HepG2 cells, followed by treatment of DA in a dose-dependent manner as indicated. All the experiments were done in triplicates. For analysis one-way ANOVA was used, bar graphs are mean ± s.e.m. $^{**}P < 0.01$, $^{***}P < 0.001$

factors- lymphoid enhancer-binding factor (LEF) and T-cell factor (TCF), that consequently leads to the expression of its target genes including cyclin D1 [25, 26]. Cyclin D1 promotes mitosis and has a prominent role in cell proliferation and survival [27]. Since dysregulation of Wnt/β-catenin signaling pathway has been observed in many cancers, small molecules that inhibit Wnt/β-catenin pathway are pursued for developing them as anti-cancer agents [28]. Many synthetic and natural product-based small molecules have been reported to inhibit Wnt/β-catenin signaling in in vitro model systems. Natural products such as salinomycin, nigericin, silibinin and prodigiosin have been shown to inhibit Wnt/β-catenin signaling in cancer cell lines [8, 29, 30].

Recently, we isolated dinactin from *Streptomyces puniceus* and analyzed its anti-cancer effects. Dinactin and salinomycin are both ionophore antibiotics. Since, salinomycin is shown to inhibit Wnt/β-catenin signaling and down-regulate the expression of Wnt target genes, we anticipated dinactin might be inhibiting Wnt/β-catenin signaling as well. Thus, in our first set of experiments, we determined the anti-proliferative effects of dinactin on a panel of cancer cell lines. Dinactin exhibited potent growth inhibitory activity against human cancer cell lines in a dose-dependent manner; however, we did not observe any cell death in a normal cell line, HEK-293 cells, even up to 80 μM. We then analyzed the mechanism of dinactin-mediated cell death in HCT-116 cells by immunoblotting caspase-3 and parp-1 proteins, and showed the effect was independent of apoptosis. Furthermore, we observed that the growth inhibitory effects of dinactin were mediated by cell cycle arrest of HCT-116 cells in G1 phase. The G1 arrest by dinactin correlated with the down-regulation of cyclin D1 and a significant increase in the levels of p21—a negative regulator of G1 transition and also a negative regulator of cyclin D1. Since dinactin treatment caused a significant decrease in cyclin D1 activity and the fact

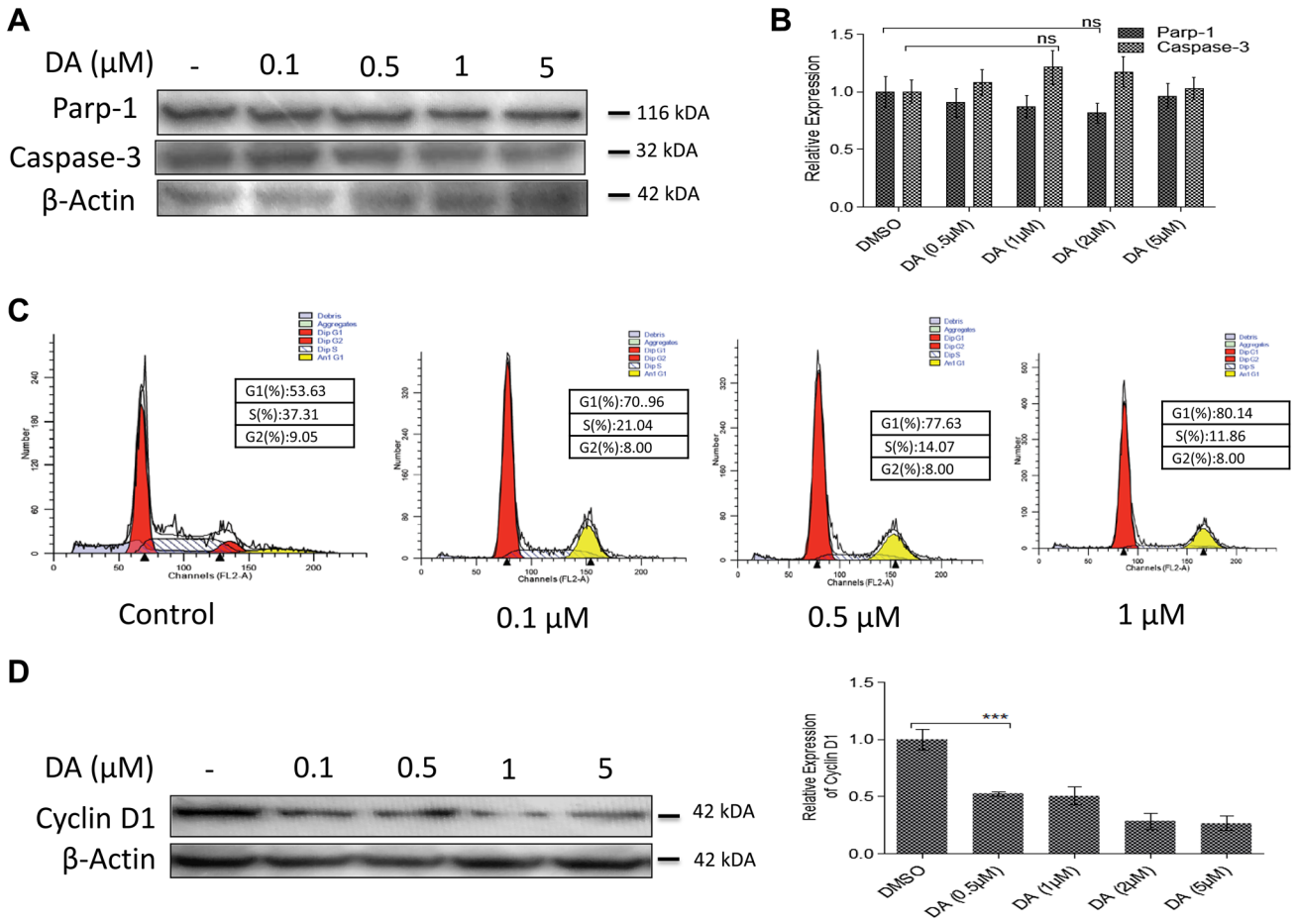

Fig. 5 Dinactin inhibits proliferation of HepG2 cells through a similar mechanism as in HCT-116 cells. **a** Immunoblotting of HepG2 cell lysates using parp-1 and caspase-3 antibodies, β-actin was used as a loading control. **b** Densitometric analysis of protein expression. **c** HepG2 Cells were treated with dinactin for 24 h. Cells were stained with PI and analyzed for cell populations using flow cytometry as described in "Materials and methods". **d** Immunoblotting of HepG2 cell lysates using cyclin D1 antibodies, β-actin was used as a loading control. All the experiments were done in triplicates in HepG2 cells. For analysis one-way ANOVA was used, and bar graphs are mean ± s.e.m. $***P < 0.001$, ns denotes the non-significant

that cyclin D1 is a direct target gene of Wnt/β-catenin signaling. We analyzed the impact of dinactin on Wnt/β-catenin activity in colon and liver cancer cells, two cancers primarily resulting from dysregulated Wnt/β-catenin signaling. Thus, we carried out Top-Flash reporter activities in HCT-116 and HepG2 cells to examine the impact of dinactin on Wnt/β-catenin signaling activity. While the salinomycin significantly decreased Top-Flash activity in micro-molar concentrations, dinactin treatment caused a dose-dependent decrease in the Top-Flash reporter activity in lower nano-molar concentrations in both these cell lines suggesting that decreased cyclin D1 might be probably through inhibition of Wnt/β-catenin signaling. These data suggest that dinactin could be developed as an effective drug for the management of neuropathic pain and as prospective anti-cancer agent to substantially reduce the β-catenin activity and expression of its downstream protein cyclin D1.

Acknowledgements This work was supported by a grant from the Council of Scientific and Industrial Research (CSIR), Government of India, New Delhi, under Network Project HCP-0008. M.S.D. acknowledges CSIR-UGC for the fellowship. This manuscript represents IIIM communication number IIIM/2255/2018.

Compliance with ethical standards

Conflict of interest All authors declare that there is no conflict of interest.

Ethical approval The study was approved by the local institute committee.

References

1. Kohanski MA, Dwyer DJ, Collins JJ (2010) How antibiotics kill bacteria: from targets to networks. Nat Rev Microbiol 8:423–435
2. Galm U, Hager MH, Van Lanen SG, Ju J, Thorson JS, Shen B (2005) Antitumor antibiotics: bleomycin, enediynes, and mitomycin. Chem Rev 105:739–758
3. Hussain A, Rather MA, Dar MS, Dangroo N, Aga MA, Shah AM, Ahmad Z, Dar MJ, Hassan QP (2018) *Streptomyces puniceus* strain AS13., production, characterization and evaluation of bioactive metabolites: a new face of dinactin as an antitumor antibiotic. Microbiol Res 207:196–202
4. Žižka Z (1998) Biological effects of macrotetrolide antibiotics and nonactic acids. Folia Microbiol 43:7–14
5. Kusche BR, Smith AE, McGuirl MA, Priestley ND (2009) Alternating pattern of stereochemistry in the nonactin macrocycle is required for antibacterial activity and efficient ion binding. J Am Chem Soc 131:17155–17165
6. Izatt RM, Bradshaw JS, Nielsen SA, Lamb JD, Christensen JJ, Sen D (1985) Thermodynamic and kinetic data for cation-macrocycle interaction. Chem Rev 85:271–339
7. Borrel MN, Pereira E, Fiallo M, Garnier-Suillerot A (1994) Mobile ionophores are a novel class of P-glycoprotein inhibitors. FEBS J 223:125–133
8. Lu D, Choi MY, Yu J, Castro JE, Kipps TJ, Carson DA (2011) Salinomycin inhibits Wnt signaling and selectively induces apoptosis in chronic lymphocytic leukemia cells. Proc Natl Acad Sci 108:13253–13257
9. Huczyński A, Janczak J, Antoszczak M, Wietrzyk J, Maj E, Brzezinski B (2012) Antiproliferative activity of salinomycin and its derivatives. Bioorg Med Chem Lett 22:7146–7150
10. Felipe de Sousa EM, Vermeulen L, Richel D, Medema JP (2011) Targeting Wnt signaling in colon cancer stem cells. Clin Cancer Res 17(4):647–653
11. Ormanns S, Neumann J, Horst D, Kirchner T, Jung A (2014) WNT signaling and distant metastasis in colon cancer through transcriptional activity of nuclear β-Catenin depend on active PI3 K signaling. Oncotarget 5:2999
12. Dar MS, Singh P, Mir RA, Dar MJ (2017) Beta-catenin N-terminal domain: an enigmatic region prone to cancer causing mutations. Mutat Res 773:122–133
13. Harrison C (2013) A new player in neuropathic pain pathogenesis. Nat Rev 12:422–423
14. Itokazu T, Hayano Y, Takahashi R, Yamashita T (2014) Involvement of Wnt/β-catenin signaling in the development of neuropathic pain. Neurosci Res 79:34–40
15. Eidet JR, Pasovic L, Maria R, Jackson CJ, Utheim TP (2014) Objective assessment of changes in nuclear morphology and cell distribution following induction of apoptosis. Diagn Pathol 1:92
16. Kang M, So E, Simons A, Spitz D, Ouchi T (2012) DNA damage induces reactive oxygen species generation through the H2AX-Nox1/Rac1 pathway. Cell Death Dis 3:e249
17. Manivasagan P, Venkatesan J, Sivakumar K, Kim S-K (2014) Pharmaceutically active secondary metabolites of marine actinobacteria. Microbiol Res 169:262–278
18. Zothanpuia AKP, Chandra P, Leo VV, Mishra VK, Kumar B, Singh BP (2017) Production of potent antimicrobial compounds from *Streptomyces cyaneofuscatus* associated with fresh water sediment. Front Microbiol 8:68
19. Dar MS, Singh P, Singh G, Jamwal G, Hussain SS, Rana A, Akhter Y, Monga SP, Dar MJ (2016) Terminal regions of β-catenin are critical for regulating its adhesion and transcription functions. Biochim Biophys Acta (BBA)-Mol Cell Res 1863:2345–2357
20. Jamwal G, Singh G, Dar MS, Singh P, Bano N, Syed SH, Sandhu P, Akhter Y, Monga SP, Dar MJ (2018) Identification of a unique loss-of-function mutation in IGF1R and a crosstalk between IGF1R and Wnt/β-catenin signaling pathways. Biochim Biophys Acta Mol Cell Res 1865(6):920–931
21. Fuchs D, Heinold A, Opelz G, Daniel V, Naujokat C (2009) Salinomycin induces apoptosis and overcomes apoptosis resistance in human cancer cells. Biochem Biophys Res Commun 390:743–749
22. Moon RT, Kohn AD, De Ferrari GV, Kaykas A (2004) WNT and β-catenin signalling: diseases and therapies. Nat Rev Genet 5:691–701
23. Dihlmann S, von Knebel Doeberitz M (2005) Wnt/β-catenin-pathway as a molecular target for future anti-cancer therapeutics. Int J Cancer 113:515–524
24. Polakis P (2007) The many ways of Wnt in cancer. Curr Opin Genet Dev 17:45–51
25. He T-C, Sparks AB, Rago C, Hermeking H, Zawel L, da Costa LT, Morin PJ, Vogelstein B, Kinzler KW (1998) Identification of c-MYC as a target of the APC pathway. Science 281:1509–1512
26. Tetsu O, McCormick F (1999) β-Catenin regulates expression of cyclin D1 in colon carcinoma cells. Nature 398:422–426
27. Kalani MYS, Cheshier SH, Cord BJ, Bababeygy SR, Vogel H, Weissman IL, Palmer TD, Nusse R (2008) Wnt-mediated self-renewal of neural stem/progenitor cells. Proc Natl Acad Sci 105:16970–16975
28. Kahn M (2014) Can we safely target the WNT pathway? Nat Rev Drug Discovery 13:513–532
29. Lu W, Lin C, King TD, Chen H, Reynolds RC, Li Y (2012) Silibinin inhibits Wnt/β-catenin signaling by suppressing Wnt co-receptor LRP6 expression in human prostate and breast cancer cells. Cell Signal 24:2291–2296
30. Wang Z, Li B, Zhou L, Yu S, Su Z, Song J, Sun Q, Sha O, Wang X, Jiang W (2016) Prodigiosin inhibits Wnt/β-catenin signaling and exerts anticancer activity in breast cancer cells. Proc Natl Acad Sci 113:13150–13155